Published in final edited form as:

J Immunol. 2017 January 01; 198(1): 452–460. doi:10.4049/jimmunol.1601346.

Critical role of LTB4/BLT1 in IL-23 induced synovial inflammation and osteoclastogenesis via NF-κB

Laura Bouchareychas[*], **Eva M Grössinger**[*], **Mincheol Kang**[*], **Hong Qiu**[*], and **Iannis E Adamopoulos**[*,†,‡]

[*]Division of Rheumatology, Allergy and Clinical Immunology, University of California, Davis

[†]Institute for Pediatric Regenerative Medicine, Shriners Hospitals for Children Northern California, CA, USA

Abstract

IL-23 activates the synthesis and production of Leukotriene B4 (LTB4) in myeloid cells, which modulate inflammatory arthritis. In this manuscript we investigate the role of LTB4 and its receptor LTB4R1 (BLT1) in synovial inflammation and osteoclast differentiation. Specifically, we utilized IL-23 *in vivo* gene transfer to induce arthritis in mice and showed that elevated serum LTB4 and synovial expression of 5-LO correlated with increased disease severity by histological evaluation and paw swelling compared to GFP-gene transfer controls. To further investigate the effect of LTB4 pathway in bone loss we performed osteoclast differentiation assays by stimulating with M-CSF and RANKL bone marrow cells derived from $BLT1^{+/+}$ and/or $BLT1^{-/-}$ mice and utilized qPCR for gene expression analysis in terminally differentiated osteoclasts. Deficiency in BLT1 resulted in the up-regulation of osteoclast related genes and an increase in the formation of giant, multi-nucleated $TRAP^{+}$ cells capable of F-actin ring formation. In addition, BLT1 deficiency showed an increase of phosphorylated NF-κB and phosphorylated IκB levels in osteoclasts. We also performed real time calcium imaging to study the effect of BLT1 deficiency in RANKL-induced activation of intracellular calcium flux *in vitro*. Our data show that LTB4 and its receptor BLT1 exacerbate synovial inflammation *in vivo* and bone resorption *in vitro* suggesting LTB4 and BLT1 could be effectively targeted for the treatment of musculoskeletal diseases.

Keywords

Osteoclasts; inflammatory arthritis; Leukotriene; Interleukin 23

[‡]Correspondence and reprint requests to Iannis E Adamopoulos, Shriners Hospital for Children Northern California, Institute for Pediatric Regenerative Medicine, 2425 Stockton Blvd, Room 653A, Sacramento, CA 95817. iannis@ucdavis.edu Tel: 916-453-2237, Fax: 916-453-2000.

Disclosures

The authors have no financial conflicts of interest.

Author's Contributions

LB performed the in vivo experiments, immunofluorescence, osteoclast assays, and statistical analysis and wrote the manuscript. EG performed the calcium measurements. MK performed the western blotting experiments. HQ performed histologic analysis. IEA supervised and coordinated all the experiments and wrote the manuscript. All authors read and approved the final manuscript.

Introduction

Interleukin-IL23 (IL-23) and Leukotriene B4 (LTB4) are two mediators that are known to play separately major roles in the pathogenesis of several autoimmune/inflammatory diseases including Rheumatoid arthritis (RA). They are both found elevated in the serum, synovial fluid of patients with RA, and participate in the induction of pro-inflammatory cytokines that cause further damage to the joints (1, 2). IL-23 is a pro-inflammatory cytokine produced by innate immune cells and is well known to be essential for the T lymphocyte differentiation through IL-23R signaling (3, 4). IL-23 has been implicated in mediating inflammatory bone loss (5, 6) attributable to excessive bone resorption by osteoclasts.

Osteoclasts are giant, multinucleated, bone-degrading cells derived from monocyte/macrophage precursor cells and develop into fully functional osteoclasts upon macrophage colony-stimulating factor (M-CSF) and receptor activator of nuclear factor κB ligand (RANKL) activation (7). M-CSF is crucial for the proliferation and survival of precursor cells of osteoclasts, mainly by activating ERK (extracellular-signal-regulated kinase) and AKT through PI3K (phosphoinositide 3-kinase) (8). A series of genetically modified mice has clearly shown that RANKL-RANK signaling plays a pivotal role in osteoclastogenesis and osteoclast function (9, 10). The crucial target of signaling by RANKL is activation of TRAF6 (TNF receptor-associated factor 6), which leads to the activation of nuclear factor kappa B (NF-κB) and mitogen-activated kinases (MAPKs), including JUN N-terminal kinase (JNK) and p38 (11). NF-κB protein is sequestered in the cytoplasm in normal states forming a complex with inhibitor κB (IκB). RANKL is able to induce the phosphorylation of IκB, which is a prerequisite to NF-κB cascade activation (12). Active NF-κB translocates to the nucleus and activates the osteoclast differentiation transcription factors c-fos and nuclear factor of activated *T*-cells cytoplasmic 1 (NFATc1), which collectively orchestrate the transcription of osteoclast related genes including tartrate resistant acid phosphatase 5, (*Acp5*), matrix metallopeptidase-9 (*Mmp9*), and cathepsin K (*Ctsk*) (13).

IL-23 has been shown to promote human and mouse osteoclast formation *in vitro* (14–16). We recently described a new role of IL-23 in activating the synthesis and production of LTB4 in innate immune cells, essential to orchestrate osteoclast differentiation and activation in inflammatory arthritis (17). Moreover we showed that LTB4 activates significant calcium flux on osteoclast precursors, which is known to augment osteoclastogenesis (13, 16). Furthermore, IL-23 cross-talk with ITAM-immunoreceptors induces calcium signaling which are also involved in activating the leukotriene biosynthesis pathway (16).

LTs are produced predominantly by inflammatory cells at the nuclear envelope in response to a wide range of stimuli. They are generated by the release of arachidonic acid (AA) from membrane phospholipids through the action of cytosolic phospholipase A2 (cPLA2). AA is first oxidized into 5-hydroperoxyeicosatetraenoic acid (5-HPETE) and then in leukotriene A4 (LTA4) by the 5-lipoxygenase (5-LO) and 5-lipoxygenase-activating protein (FLAP) complex. Depending on the cellular enzymes present and cell specificity, the LT cascade branches to LTB4 or LTC4 synthesis (18, 19). The action of LTB4 is mediated through two seven-pass transmembrane G-protein coupled receptor (GPCRs). LTB4 activates, high and

low-affinity receptors, LTB4 receptor type-1 (BLT1) and LTB_4 receptor type-2 (BLT2) respectively (20, 21). The leukotriene biosynthetic pathways and LTB4 receptors plays an important role in the development of inflammatory arthritis (22, 23). BLT1-deficient mice are resistant to both K/BxN serum transfer arthritis and collagen-induced arthritis and BLT1 inhibitor, CP-105,696 is sufficient to offer complete protection of mice from developing arthritis (24, 25). *In vitro* and *in vivo* studies demonstrated that LTB4 could directly stimulate osteoclast differentiation in mouse and human (26) and bone resorption in mouse (27). Therefore, elucidating the LTB4/BLT1 axis regulatory mechanisms of the differentiation and activation of osteoclasts is critical for an improved understanding of pathological bone loss. Despite this strong indications in animal models clinical trial of a LTB4 receptor antagonist, (BIIL 284), in patients with rheumatoid arthritis produced only modest improvements in disease activity based on ACR scores, and unfortunately the structural bone damage was not evaluated (28).

In this study, we identified critical roles for BLT1 in IL-23 induced myelopoiesis and osteoclastogenesis. We demonstrated that systemic overexpression of IL-23 increase LTB4 serum levels compared to control mice and increase the expression of key enzymes in LTB4 synthesis pathway in the synovium. Furthermore, we observed that $BLT1^{-/-}$ mice are more potent to osteoclast formation than $BLT1^{+/+}$ due to an increase of phosphorylated NF-κB and phosphorylated IκB levels and higher calcium activity in osteoclast. Collectively our results highlight a negative regulatory role of BLT1 in RANKL-induced osteoclastogenesis and the associated inflammatory bone loss.

Method

Reagents and mice

B10.RIII [B10.RIII-H2r H2-T18b/(71NS)SnJ], $BLT1^{-/-}$ [B6.129S4-*Ltb4r1tm1Adl*/J;(29)] and strain-matched $BLT1^{+/+}$ C57BL/6 mice were purchased from Jackson Laboratories (Sacramento, CA, USA), breed and raised in the same facility with identical specific pathogen–free conditions. The University of California at Davis Institutional Animal Care and Use Committee approved all animal protocols. LTB4 measurement was performed according to the protocol described in the LTB4 EIA protocol by Cayman Chemicals (LTB4 EIA kit, Cayman Chemicals Ltd., Michigan, USA). Serum IL-23 was assayed using an ELISA purchased from BioLegend in accordance with the manufacturer's instructions. Flow cytometry anti-mouse CD16/32 (93), CD11b (M1/70), Ly-6C (HK1.4), Ly-6G (1A8) and CD115 (AFS98) were all purchased from BioLegend (San Diego, USA). All cell incubations were performed in culture medium consisting of αMEM with 2mM L-glutamine, 10% heat-inactivated FBS, 100 IU/ml Penicillin and 100 IU/ml Streptomycin (Life Technologies). Mouse soluble M-CSF and RANKL were purchased from R & D Systems, Inc (Minneapolis, USA). AlamarBlue solution (Life Technologies) was used for cell viability assay. The phospho-AKT (D9E), total AKT (C67E7), phospho-ERK1/2 (D13.14.4E), total ERK1/2 (3A7), phospho-IκBα (14D4), total IκBα (44D4), Phospho-NF-κB (93H1), total NF-κB (C22B4), were all purchased from Cell signaling (Cell signaling, USA). IRDye 800CW Donkey anti-Rabbit IgG (H + L) and IRDye 680LT Donkey anti-Mouse IgG (H + L) were all purchased from LICOR Biosciences.

Microarray Analysis

Total RNA was amplified and purified using an Ambion Illumina RNA amplification kit (Ambion) to yield biotinylated cRNA and 1.5 μg of cRNA samples were hybridized to Illumina WG-6 v2.0 chips according to manufacturer's instructions. Arrays were scanned by Illumina iScan. Raw data were extracted using the software provided by the manufacturer (Illumina GenomeStudio) analyzed and deposited in NCBI GEO under assesion number: GSE86998, http://www.ncbi.nlm.nih.gov/geo/query/acc.cgi?acc=GSE86998

Production and purification of GFP and IL-23 minicircle DNA and hydrodynamic delivery

Minicircle-RSV.Flag.mIL23.elasti.bpA or RSV.eGFP.bpA was produced as described by Chen et al (30). A single isolated colony from a fresh plate was grown for 8 h in 2 ml Luria-Bertani broth with kanamycin. Eight hundred microliters of this culture was used to inoculate 1L Terrific broth and grown for an additional 17 h. Overnight cultures were centrifuged at 20°C, 4000 rpm for 20 min. The pellet was resuspended 4:1 (v/v) in fresh Luria-Bertani broth containing 1% L-arabinose. The bacteria were incubated at 32°C with constant shaking at 250 rpm for 2 h. After adding half volume of fresh low-salt Luria-Bertani broth (pH 8.0) containing 1% L-arabinose, the incubation temperature was increased to 37°C and the incubation continued for an additional 2 h. Episomal DNA circles were prepared from bacteria using plasmid purification kits from Endofree Qiagen Megaprep (Chatsworth, CA, USA). Hydrodynamic delivery of MC DNA using the tail vein was performed as previously described, resulting in stable overexpression of IL-23 for a period of at least 90 days (6).

Evaluation of Arthritic Clinical Score

Disease severity for each limb is recorded as follows: 0 = normal; 1 = erythema and swelling of one digit; 2 = erythema and swelling of two digits 3 = erythema and swelling of more than two digits and/or swelling ankle joint. The clinical arthritis score is defined as the sum of the scores for all four paws of each mouse.

Immunohistochemistry

Immunohistochemistry staining of 5-LO was performed at day 14 on formalin-fixed paraffin-embedded joint tissues collected from GFP MC and IL-23 MC B10.RIII injected mice. Paraffin slides were deparaffinized using xylene and serial alcohol, and decalcified using Decalcifier I solution (Leica Biosystems) according to manufacturer's instructions. The slides were immunostained using primary anti-5-LO antibody (abcam #39347, 1:100) or anti-rabbit IgG isotype control at 4°C overnight, followed by incubation using biotin-labeled secondary (Sigma 1:800) for 1 hour at RT, and Advanced avidin/biotin staining system (Vector Laboratories), according to manufacturer's instructions. Images were acquired using C1 confocal microscope (Nikon).

Mouse osteoclast assays

Osteoclasts were differentiated from bone marrow cells as previously described (6). Briefly, hematopoietic bone marrow cells were flushed from tibia and femurs of 8–12-week-old $BLT1^{+/+}$ and $BLT1^{-/-}$ mice. Cells were differentiated with 25 ng/ml of mouse M-CSF for 2

days, then with 25 ng/ml of mouse M-CSF and 30 ng/ml of mouse sRANKL for 2, 4 or 6 days as indicated in individual experiments. Mature osteoclasts were identified microscopically and cytochemically as multinucleated (more than three nuclei) TRAP cells using a commercially available kit (Sigma-Aldrich). Functional assessment of osteoclast formation was performed using F-actin staining, cells were incubated with TRITC-conjugated phalloidin (Sigma-Aldrich) for 20 min. Images were acquired using A1 confocal microscope (Nikon).

RNA extraction and real-time quantitative PCR

Osteoclast differentiation was quantified by the RNA expression of osteoclast marker genes using reverse-transcription quantitative PCR. Total RNA was purified using the RNeasy Mini Kit (Qiagen). RNA preparation was reverse-transcribed using Omniscript RT Kit (Qiagen). The resultant cDNA were amplified by qPCR using Brilliant III Ultra-Fast SYBR QPCR (Agilent technologies) with the following primers: Mouse *B2m*, 5′-CTGCTACGTAACACAGTTCCACCC-3′ and 5′-CATGATGCTTGATCACATGTCTCG-3′; mouse *Nfatc1*, 5′-TTGCGGAAAGGTGGTATCTC-3′ and 5′-TGGGAGATGGAAGCAAAGAC-3′; mouse *Ctsk*, 5′-AAGTGGTTCAGAAGATGACGG-3′ and 5′-TCTTCAGAGTCAATGCCTCCG-3′; mouse *Acp5*, 5′-AGCAGCCAAGGAGGACTACGT-3′ and 5′-TCGTTGATGTCGCACAGAGG-3′; mouse *Mmp9*, 5′-AATCTCTTCTAGAGACTGGGA-3′ and 5′-AGCTGATTGACTAAAGTAGCT-3′; and mouse *Calcr*, 5′-GCCTCCCCATTTACATCTGC-3′ and 5′-CTCCTCGCCTTCGTTGTTG-3′. Experiments were performed 3 times, in triplicate wells. Data elaboration was performed as relative quantification analysis using the $2^{-\Delta\Delta CT}$ method. Data were normalized with an internal *B2m* control. Gene expression was expressed relative to the control M-CSF group gene expression profile.

Flow cytometry

Blood samples were collected in EDTA tubes (Sarstedt) from tail bleeds and labeled with leucocyte-specific antibodies as previously described (31). Red blood cells were lysed by ACK (Life Technologies). Non-specific binding was blocked with TruStain FcX antibody for 10 min at 4 °C in FACS buffer (Ca^{2+}/Mg^{2+}-free PBS with 0.5% BSA), before staining with appropriate antibodies CD11b (1:200), Ly-6C (1:800), Ly-6G (1:1000) and CD115 (1:500). Cells and beads (polyscience) were counted on an Attune Cytometer (Life Technologies) and analyzed using FlowJo software (Tree Star, Ashland, OR, USA).

Calcium imaging

Bone marrow cells from $BLT1^{+/+}$ and $BLT1^{-/-}$ mice were isolated, plated onto 35 mm petri dishes and differentiated into osteoclasts as described above. After 48 hours of stimulation in the presence or absence of 30 ng/mL RANKL, macrophages and osteoclasts were loaded with the calcium-sensitive dye Fluo-4-AM at 2.5 μM (Molecular probes) including 0.1% Pluronic F-127 (Invitrogen) for 30 min on 37°C in their culture medium. Prior to imaging with a confocal upright microscope (Nikon), cells were washed with medium and then incubated for another 15 min in their respective culture medium including all supplements

including MCSF +/− RANKL in the absence of phenol red. Ca^{2+}-induced fluorescence in cells was recorded in time-lapse videos in this medium, in a 1-second interval mode for a total duration of 5 min and interpreted using NIS-Elements BR software (Nikon Instruments, NY, USA) and Microsoft excel (Microsoft).

Western Blot and phosphorylation studies

Bone marrow derived macrophages and osteoclasts cells were lysed in a RIPA buffer (cell signaling) with phosphatase inhibitors (Pierce) and Mini EDTA-free Protease Inhibitor Cocktail (Roche). Insoluble material was removed by centrifugation at 13,000g for 20 minutes at 4°C. Final protein concentrations were determined using BCA protein assay kit (Pierce). Electrophoresis was performed using 4~15% Mini-PROTEAN TGX Precast Gels (Bio-Rad) and the blots were transferred to PVDF membranes (EMD Millipore). After 1 h of blocking with 5% BSA membranes were incubated overnight at 4 °C using appropriate primary antibodies. Membranes were incubated with IRDye rabbit and mouse secondary antibodies (1:10000) (LICOR Biosciences) for 1 h protected from light. Membranes were scanned using an Odyssey Imaging System and analyzed with Odyssey v2.0 software (LICOR Biosciences). Time dependent phosphorylation experiments were performed in total cell lysates isolated from bone marrow derived macrophages for M-CSF studies and osteoclasts for RANKL studies. Cells were serum starved using serum free medium for at least 8 hours prior to stimulation with 100ng/ml M-CSF or 100ng/ml RANKL and total cell lysates were collected after 0, 5, 15, 30, and 60 minutes.

Statistical analysis

Statistical tests included unpaired, two-tailed Student's *t* test, Mann-Whitney test or ANOVA where appropriate as indicated in individual figure legends. A *P* value of 0.05 or less was considered to denote significance.

Results

Hydrodynamic delivery of IL-23 MC induces LTB4 synthesis *in vivo* and inflammatory arthritis

IL-23 was overexpressed in 10–12-week-old B10.RIII male mice using minicircle DNA (IL-23 MC) by hydrodynamic tail vein injection to investigate whether IL-23 affects the expression of the potent chemoattractant and pro-inflammatory mediator LTB4. Control groups included mice injected with equal amounts of GFP minicircle DNA (GFP MC). To quantify serum IL-23, blood samples were collected 3 days after the injection. IL-23 MC injected mice revealed a significant elevation of serum IL-23 whereas GFP MC injected mice did not have detectable levels of IL-23 (Fig. 1A). Interestingly, 7 days after IL-23 MC injection we observed an increase in serum LTB4 (Fig. 1B).

The increased expression of IL-23 and LTB4 in IL-23 injected mice was associated with joint swelling and erythema of the front and hind paws (Fig. 1C) with a maximum incidence of 71% (Fig. 1D), which was completely absent in mice treated with GFP MC. Representative images of hind paws from both experimental groups at the end of the experiment are shown in Fig. 1C, 1E.

Histological analysis of the ankle joints, 14 days after GFP or IL-23 MC injection, showed that 5-LO, a key enzyme in LTB4 synthesis was abundantly expressed in the joints of IL-23 MC injected mice compared to control mice as indicated by dark brown precipitate (Fig. 1G, 1H). Furthermore, haematoxylin staining demonstrated that joints of IL-23 MC injected mice had cellular infiltrates within the joint space (Large arrow) and infiltrating pannus containing 5-LO expressing cells (small black arrows). Collectively our data provide novel evidence that 5-LO, which plays a critical role in the biosynthesis of LTB4, is associated with IL-23 induced synovial inflammation.

IL-23 expression induces myelopoiesis independently of BLT1 pathway

Since the LTB4-BLT1 pathway is involved predominantly in myeloid recruitment into the joint (22, 24), we examined whether BLT1 deficiency affect neutrophil and monocyte population in peripheral blood by flow cytometry analysis post IL-23 gene-transfer. We performed gated analysis of both monocyte subsets namely $CD115^{+}$ $Ly\text{-}6C^{low}$ (a) and $CD115^{+}$ $Ly\text{-}6C^{hi}$ (b) and a neutrophil population detected in the $CD115^{-}$ $Ly\text{-}6C^{+}$ and $CD11b^{+}$ $Ly\text{-}6G^{+}$ (c) in $BLT1^{+/+}$ mice (Fig. 2A). We performed the same gating strategy in the $BLT1^{-/-}$ mice (Fig. 2B) and our direct comparison two days after IL-23 MC injection, revealed an expansion of the monocytes in the blood of both $BLT1^{+/+}$ (Fig. 2C) and $BLT1^{-/-}$ mice (Fig. 2E) compared to GFP MC. In both $BLT1^{+/+}$ and $BLT1^{-/-}$ mice, the proportion of $Ly\text{-}6C^{hi}$ monocytes is increased in IL-23 gene transfer but not the $Ly\text{-}6C^{low}$ monocytes. Moreover, the total number of circulating neutrophils was significantly higher with IL-23 MC compared with GFP MC in $BLT1^{-/-}$ as well as in $BLT1^{+/+}$ mice (Fig. 2D and F). We performed identical analysis to bone marrow populations where we show that there is no difference (Supplementary Fig. 1). Taken together, these data demonstrate that inflammatory monocytes and neutrophils are equally increased after IL-23 gene transfer between $BLT1^{+/+}$ and $BLT1^{-/-}$ mice and demonstrate that genetic ablation of BLT1 receptor does not influence myeloid egression from the bone marrow to peripheral blood.

BLT1 deficient mice show increased osteoclast differentiation

LTB4/BLT1 related genes are expressed in monocyte/macrophage (32, 33) osteoclast precursors, however little is known about their expression and function in osteoclasts. To further study the role of BLT1 on myeloid cells, we performed DNA microarray analysis on macrophages and terminally differentiated osteoclasts and specifically analyzed the expression of genes that regulate LTB4 synthesis and signaling namely Alox12 (arachidonate 12-lipoxygenase), Alox15 (arachidonate 15-lipoxygenase), Alox5 (arachidonate 5-lipoxygenase), Alox5ap (arachidonate 5-lipoxygenase activating protein), Alox8, (arachidonate 8-lipoxygenase), Lta4h (leukotriene A4 hydrolase), Ltb4r1 (leukotriene B4 receptor 1), Ltb4r2 (leukotriene B4 receptor 2), Ltc4s (leukotriene C4 synthase). From this selection of LTB4 synthesis and signaling related genes, we observed that only Ltb4r1 (BLT1) expression decreased by more than 2 fold between macrophages (Mφ) and osteoclasts (OC) (Fig. 3A and 3B). However Ltb4r2 (BLT2) expression was not different in macrophages compared to osteoclasts, also confirmed by real-time PCR (data not shown). These results suggest a more important role of BLT1 in RANKL-induced osteoclast differentiation compared to BLT2.

To address any potential functional significance we performed osteoclastogenesis assays derived from BLT1$^{+/+}$ and BLT1$^{-/-}$ bone marrow cells. We observed that mouse osteoclast precursors successfully differentiated into large (100–300 um) multinucleated TRAP^{+} osteoclasts after a total of 6 days of M-CSF and RANKL treatment in both BLT1$^{+/+}$ and BLT1$^{-/-}$ cells (Fig. 3C). Interestingly the number of TRAP^{+} multinucleated cells was significantly increased in BLT1$^{-/-}$ mice ($p<0.05$) (Fig. 3D). BLT1$^{+/+}$ and BLT1$^{-/-}$ osteoclasts exhibited normal F-actin ring shown in RANKL treated cultures (Fig. 3E). Together, these results shows that the BLT1$^{-/-}$ bone marrow cells are able to differentiate into mature osteoclasts and have an increased potential to osteoclast formation. To determine at which stage of osteoclast differentiation BLT1 plays a role, we performed real-time qPCR analysis in bone marrow cells cultured with M-CSF and stimulated with RANKL for 4 days. We found that *Acp5, Ctsk* and *Mmp9* mRNA levels were significantly increased in BLT1 deficient osteoclasts compared to BLT1$^{+/+}$ osteoclasts (Fig. 3F, 3G, 3H). *Calcr* showed an increasing trend that did not reach significance (Fig. 3I). Interestingly *Ctsk* and *Mmp9* were significantly elevated even at the earlier time-point of day 2 in BLT1$^{-/-}$ compared to BLT1$^{+/+}$ osteoclasts (Supplementary Fig. 2) suggesting that BLT1 signaling may play a role in cell differentiation program of osteoclasts rather than its activation. M-CSF stimulation, showed no statistical differences between BLT1$^{-/-}$ and BLT1$^{+/+}$ cells. Consistent with the suspected role of BLT1 in RANKL-induced osteoclast differentiation, we observed that osteoclast related genes increased in BLT1$^{-/-}$ osteoclasts compared to BLT1$^{+/+}$ suggesting that BLT1 may suppress osteoclast differentiation.

BLT1$^{-/-}$ mice exhibit increased RANKL-induced NF-κB activity

To gain insight into the mechanism by which BLT1 modulates osteoclast differentiation, we investigated the effects of M-CSF and RANKL signaling in downstream effectors and transducers and performed cell viability assays. Specifically we performed cell viability assays in bone marrow cells isolated from BLT1$^{+/+}$ and BLT1$^{-/-}$ mice in day 2, 4 and 6 after RANKL stimulation. Although we observed that BLT1$^{-/-}$ bone marrow cells at day 2 had a slightly decreased number of viable cells compared to BLT1$^{+/+}$ cells, it did not affect the cell viability at day 4 and day 6 after RANKL stimulation which was when we performed our assays (Fig. 4A). To further investigate the M-CSF survival pathway we performed Western blotting on total cell lysates stimulated with M-CSF (100ng/ml), at different time points and measured the activation of ERK and Akt signaling implicated in regulation of osteoclast precursor survival and proliferation. We observed no differences between BLT1$^{+/+}$ and BLT1$^{-/-}$ bone marrow macrophages in AKT and ERK1/2 signaling activation (Fig. 4B). To determine the influence of BLT1 deficiency in osteoclast differentiation pathways we performed Western blotting on total cell lysates stimulated with RANKL (100ng/ml), at different time points and measured the phosphorylation of IκBα, and NF-κB (Fig. 4C). Our data showed a significant increase of phosphorylated IκBα levels, which were also accompanied by an up-regulation of NF-κB levels in BLT1$^{-/-}$ compared to BLT1$^{+/+}$ osteoclasts. The enhanced RANKL-induced phosphorylation of NF-κB pathway in BLT1 deficient mice is in keeping with an inhibitory role of BLT1 on RANKL-induced NF-κB signaling pathway during osteoclastogenesis.

Increased calcium activity in RANKL-stimulated BLT1$^{-/-}$ macrophages

To investigate the intracellular signaling pathways that involve BLT1 in osteoclast formation, we performed calcium-imaging experiments. Quantitative and qualitative properties of cells displaying Ca^{2+} oscillation-like patterns were analyzed in response to M-CSF +/− RANKL for 48 h in bone marrow macrophages derived from BLT1$^{+/+}$ and BLT1$^{-/-}$ mice (Fig. 5). Whereas macrophages stimulated with M-CSF and loaded with Fluo-4-AM exhibited similar Ca^{2+} activity between BLT1$^{+/+}$ and BLT1$^{-/-}$ (Fig. 5C), RANKL stimulation significantly increased the relative number of responding cells in BLT1$^{-/-}$ compared to BLT1$^{+/+}$samples (Fig. 5D). However, the number of Ca^{2+} transients in those responding cells remains unchanged between the two groups (Fig. 5E). Taken together these data emphasize that BLT1 deficiency increases the relative number of cells that show calcium signaling in response to RANKL stimulation - whilst there is no qualitative difference in Ca^{2+} oscillations.

Discussion

In this study, we have reported a link between IL-23 and LTB4 synthesis pathway in the pathophysiology of chronic inflammatory arthritis. We demonstrated that BLT1 is not essential to IL-23 derived myelopoiesis-induced arthritis. Furthermore we found a regulatory role of BLT1 on osteoclast differentiation via NF-κB and Ca^{2+} signaling. We described LTB4 pathways activation by IL-23 and demonstrated BLT1 regulatory role on osteoclasts differentiation in murine model of chronic inflammatory arthritis.

IL-23 overexpression in adult mice using hydrodynamic delivery of IL-23-encoding MC DNA induced high levels of LTB4 associated with abundant cellular infiltrate in the synovium expressing 5-LO. Our results suggest that LTB4 could play a critical role in the induction as well as perpetuation of arthritis by IL-23 overexpression through egression of myeloid cell populations pertinent to arthritis initiation and progression. Indeed, as a chemoattractant of monocytes and neutrophils, LTB4 might be the major mediator of joint inflammation observed in IL-23 MC injected mice. LTB4 along with the components of the LTB4 pathway (including 5-LO) are present in serum and synovial fluid from patients with active rheumatoid arthritis and its levels correlate with the disease severity (2, 34). Moreover the absence of BLT1 signaling is protective in various animal models of systemic inflammation including collagen-induced arthritis (23, 29, 35, 36).

Neutrophil infiltration into the joints is a prominent feature of mice with inflammatory arthritis. Once in the joint, neutrophils perpetuate their own recruitment by releasing LTB4 contributing to the chronicity of the disease (22). Previous studies using BLT1 deficient mice report that neutrophil expression of BLT1 was absolutely required for arthritis generation and neutrophils recruitment into the joint in K/BxN mouse model of inflammatory arthritis (24). In the present study, we report that IL-23 systemic overexpression induces the expansion of monocytes and neutrophils in the blood, independently of BLT1. Although we did not detect a reduction in myeloid cell population in the bone marrow due to the continuous induction of granulopoiesis and myelopoiesis in our gene transfer model it is evident that IL-23 plays a major role in the emigration of myeloid cells from the bone marrow to the circulation and that LTB4/BLT1 plays a major role in the recruitment of those

cells from the circulation to the joint. Interestingly, we observed an increase in circulatory pro-inflammatory Ly-6C^{hi} subtypes but not Ly-6C^{low} monocytes in mice injected with IL-23 MC compared to GFP MC. These findings may be explained by higher proliferative activity or higher kinetics of the development of Ly-6C^{hi} compared to Ly-6C^{low} monocytes (37). The process of monocyte recruitment and differentiation is still a matter of controversy. *Misharin and al.* have reported that Ly-6C^{low} monocytes are crucial for the initiation of joint inflammation and can be recruited to the joint during inflammation (38). Recently, *Dal-Secco et al* have shown in situ monocyte reprogramming in the liver, from proinflammatory Ly-6C^{hi} cells into reparative Ly-6C^{low} cells and show, that this occurs at the site of injury (39). Further studies are needed to understand monocyte plasticity within the tissue microenvironment and especially to the joint, as monocytes are known to be osteoclasts precursors.

H. Hikiji et al have previously shown by qPCR that osteoclasts expressed BLT1 mRNA but not BLT2 mRNA (40). Our DNA-microarray analysis data demonstrate that cultured macrophages and osteoclasts express both BLT1 and BLT2 mRNA. We also observed that BLT1 expression is down-regulated during macrophage to osteoclast differentiation suggesting a possible distinct role of BLT1 in osteoclastogenesis. In fact, our osteoclast differentiation experiments demonstrated that genetic ablation of BLT1 increases RANKL-induced osteoclast formation as evidenced by the formation of multinucleated TRAP^{+} cells that were capable of F-actin ring formation. Moreover, BLT1$^{-/-}$ osteoclasts presented an increase in mRNA of osteoclast-related genes *Acp5*, *Ctsk* and *Mmp9*, which facilitate bone resorption. These data are in keeping with a marked increase in RANKL-induced IkBα and NF-κB phosphorylation in BLT1$^{-/-}$ compared to BLT1$^{+/+}$ osteoclasts suggesting that BLT1 modulates RANKL signaling. Moreover, we also found an increase in the number of cells exhibiting Ca^{2+} activity in BLT1$^{-/-}$ compared to BLT1$^{+/+}$ pre-osteoclasts, which correlates with increased activation of osteoclastogenesis. Although we and others have previously shown that LTB4 signaling induces osteoclastogenesis (17, 27, 40), herein we demonstrate that BLT1 in absence of LTB4 negatively regulates osteoclast differentiation via NF-κB and Ca^{2+} signaling, thereby associating the LTB4 receptors with dual roles in osteoclastogenesis. Interestingly, others have shown that Resolvin E1 selective binding to BLT1 blocks its stimulation by LTB4 and inhibits receptor signaling and this interaction is followed by attenuation of osteoclastogenesis and resolution of acute inflammation (44). More importantly, negative regulation of osteoclastogenesis by Resolvin E1 is associated with attenuated NF-κB signaling (41). Therefore Resolvin E1 and LTB4 have counter-regulatory functions on the BLT1 receptor in determining osteoclast growth and function (41). Moreover, BLT1 is implicated in MyD88-dependent NF-κB activation macrophages (42, 43) and NF-κB activation through TLR engagement is a well-defined negative regulatory mechanism in osteoclastogenesis (44). Hence, taken together, our data show that under basal conditions, BLT1 negatively regulates osteoclastogenesis via both the activation of NF-κB, and Ca^{2+} signaling. In conclusion, a detailed mapping of crosstalk points between pro-inflammatory cytokines and lipid mediators based responses may prove paramount in the design of novel inhibitors, which can be exploited for therapeutic intervention in inflammatory arthritis and merits further investigation.

Supplementary Material

Refer to Web version on PubMed Central for supplementary material.

Acknowledgments

The authors would like to thank Drs Blythe P Durbin Johnson and Matt Lee Settles at the Bioinformatics Core in the Genome Center at UC Davis for their assistance with DNA microarray analysis.

Research reported in this publication was partly supported by SHC 250862, and the National Institute of Arthritis and Musculoskeletal and Skin Diseases of the National Institutes of Health under Award Number R01 AR062173 to IEA. EG is supported by the Austrian Science Fund (FWF): J3715-B26. The content is solely the responsibility of the authors and does not necessarily represent the official views of the National Institutes of Health.

Abbreviations used in this article

LTB4	Leukotriene B4
BLT1	Leukotriene B4 receptor 1
5-LO	5-lipoxygenase
M-CSF	Macrophage colony stimulating factor
RANKL	Receptor activator of nuclear factor kappa-B ligand
NFATC1	nuclear factor of activated *T*-cells cytoplasmic 1
ACP5	acid phosphatase 5 tartrate resistant
MMP9	matrix metallopeptidase-9
CTSK	cathepsin K
CALCR	calcitonin receptor

References

1. Kim HR, Kim HS, Park MK, Cho ML, Lee SH, Kim HY. The clinical role of IL-23p19 in patients with rheumatoid arthritis. Scand J Rheumatol. 2007; 36:259–264. [PubMed: 17763202]
2. Davidson EM, Rae SA, Smith MJ. Leukotriene B4, a mediator of inflammation present in synovial fluid in rheumatoid arthritis. Annals of the rheumatic diseases. 1983; 42:677–679. [PubMed: 6316858]
3. Parham C, Chirica M, Timans J, Vaisberg E, Travis M, Cheung J, Pflanz S, Zhang R, Singh KP, Vega F, To W, Wagner J, O'Farrell AM, McClanahan T, Zurawski S, Hannum C, Gorman D, Rennick DM, Kastelein RA, de Waal Malefyt R, Moore KW. A receptor for the heterodimeric cytokine IL-23 is composed of IL-12Rbeta1 and a novel cytokine receptor subunit, IL-23R. Journal of immunology. 2002; 168:5699–5708.
4. Ghoreschi K, Laurence A, Yang XP, Tato CM, McGeachy MJ, Konkel JE, Ramos HL, Wei L, Davidson TS, Bouladoux N, Grainger JR, Chen Q, Kanno Y, Watford WT, Sun HW, Eberl G, Shevach EM, Belkaid Y, Cua DJ, Chen W, O'Shea JJ. Generation of pathogenic T(H)17 cells in the absence of TGF-beta signalling. Nature. 2010; 467:967–971. [PubMed: 20962846]
5. Sato K, Suematsu A, Okamoto K, Yamaguchi A, Morishita Y, Kadono Y, Tanaka S, Kodama T, Akira S, Iwakura Y, Cua DJ, Takayanagi H. Th17 functions as an osteoclastogenic helper T cell subset that links T cell activation and bone destruction. The Journal of experimental medicine. 2006; 203:2673–2682. [PubMed: 17088434]

6. Adamopoulos IE, Tessmer M, Chao CC, Adda S, Gorman D, Petro M, Chou CC, Pierce RH, Yao W, Lane NE, Laface D, Bowman EP. IL-23 is critical for induction of arthritis, osteoclast formation, and maintenance of bone mass. Journal of immunology. 2011; 187:951–959.
7. Arai F, Miyamoto T, Ohneda O, Inada T, Sudo T, Brasel K, Miyata T, Anderson DM, Suda T. Commitment and differentiation of osteoclast precursor cells by the sequential expression of c-Fms and receptor activator of nuclear factor kappaB (RANK) receptors. The Journal of experimental medicine. 1999; 190:1741–1754. [PubMed: 10601350]
8. Kikuta J, Ishii M. Osteoclast migration, differentiation and function: novel therapeutic targets for rheumatic diseases. Rheumatology. 2013; 52:226–234. [PubMed: 23024017]
9. Franzoso G, Carlson L, Xing L, Poljak L, Shores EW, Brown KD, Leonardi A, Tran T, Boyce BF, Siebenlist U. Requirement for NF-kappaB in osteoclast and B-cell development. Genes & development. 1997; 11:3482–3496. [PubMed: 9407039]
10. Li J, Sarosi I, Yan XQ, Morony S, Capparelli C, Tan HL, McCabe S, Elliott R, Scully S, Van G, Kaufman S, Juan SC, Sun Y, Tarpley J, Martin L, Christensen K, McCabe J, Kostenuik P, Hsu H, Fletcher F, Dunstan CR, Lacey DL, Boyle WJ. RANK is the intrinsic hematopoietic cell surface receptor that controls osteoclastogenesis and regulation of bone mass and calcium metabolism. Proceedings of the National Academy of Sciences of the United States of America. 2000; 97:1566–1571. [PubMed: 10677500]
11. Kobayashi N, Kadono Y, Naito A, Matsumoto K, Yamamoto T, Tanaka S, Inoue J. Segregation of TRAF6-mediated signaling pathways clarifies its role in osteoclastogenesis. The EMBO journal. 2001; 20:1271–1280. [PubMed: 11250893]
12. An J, Hao D, Zhang Q, Chen B, Zhang R, Wang Y, Yang H. Natural products for treatment of bone erosive diseases: The effects and mechanisms on inhibiting osteoclastogenesis and bone resorption. International immunopharmacology. 2016; 36:118–131. [PubMed: 27131574]
13. Takayanagi H, Kim S, Koga T, Nishina H, Isshiki M, Yoshida H, Saiura A, Isobe M, Yokochi T, Inoue J, Wagner EF, Mak TW, Kodama T, Taniguchi T. Induction and activation of the transcription factor NFATc1 (NFAT2) integrate RANKL signaling in terminal differentiation of osteoclasts. Developmental cell. 2002; 3:889–901. [PubMed: 12479813]
14. Yago T, Nanke Y, Kawamoto M, Furuya T, Kobashigawa T, Kamatani N, Kotake S. IL-23 induces human osteoclastogenesis via IL-17 in vitro, and anti-IL-23 antibody attenuates collagen-induced arthritis in rats. Arthritis research & therapy. 2007; 9:R96. [PubMed: 17888176]
15. Chen L, Wei XQ, Evans B, Jiang W, Aeschlimann D. IL-23 promotes osteoclast formation by up-regulation of receptor activator of NF-kappaB (RANK) expression in myeloid precursor cells. European journal of immunology. 2008; 38:2845–2854. [PubMed: 18958885]
16. Shin HS, Sarin R, Dixit N, Wu J, Gershwin E, Bowman EP, Adamopoulos IE. Crosstalk among IL-23 and DNAX activating protein of 12 kDa-dependent pathways promotes osteoclastogenesis. Journal of immunology. 2015; 194:316–324.
17. Dixit N, Wu DJ, Belgacem YH, Borodinsky LN, Gershwin ME, Adamopoulos IE. Leukotriene B4 activates intracellular calcium and augments human osteoclastogenesis. Arthritis research & therapy. 2014; 16:496. [PubMed: 25443625]
18. Steinhilber D, Fischer AS, Metzner J, Steinbrink SD, Roos J, Ruthardt M, Maier TJ. 5-lipoxygenase: underappreciated role of a pro-inflammatory enzyme in tumorigenesis. Frontiers in pharmacology. 2010; 1:143. [PubMed: 21833182]
19. Di Gennaro A, Haeggstrom JZ. The leukotrienes: immune-modulating lipid mediators of disease. Advances in immunology. 2012; 116:51–92. [PubMed: 23063073]
20. Yokomizo T, Izumi T, Chang K, Takuwa Y, Shimizu T. A G-protein-coupled receptor for leukotriene B4 that mediates chemotaxis. Nature. 1997; 387:620–624. [PubMed: 9177352]
21. Yokomizo T, Kato K, Terawaki K, Izumi T, Shimizu T. A second leukotriene B(4) receptor, BLT2. A new therapeutic target in inflammation and immunological disorders. The Journal of experimental medicine. 2000; 192:421–432. [PubMed: 10934230]
22. Chen M, Lam BK, Kanaoka Y, Nigrovic PA, Audoly LP, Austen KF, Lee DM. Neutrophil-derived leukotriene B4 is required for inflammatory arthritis. The Journal of experimental medicine. 2006; 203:837–842. [PubMed: 16567388]

23. Griffiths RJ, Pettipher ER, Koch K, Farrell CA, Breslow R, Conklyn MJ, Smith MA, Hackman BC, Wimberly DJ, Milici AJ, et al. Leukotriene B4 plays a critical role in the progression of collagen-induced arthritis. Proceedings of the National Academy of Sciences of the United States of America. 1995; 92:517–521. [PubMed: 7831322]

24. Kim ND, Chou RC, Seung E, Tager AM, Luster AD. A unique requirement for the leukotriene B4 receptor BLT1 for neutrophil recruitment in inflammatory arthritis. The Journal of experimental medicine. 2006; 203:829–835. [PubMed: 16567386]

25. Shao WH, Del Prete A, Bock CB, Haribabu B. Targeted disruption of leukotriene B4 receptors BLT1 and BLT2: a critical role for BLT1 in collagen-induced arthritis in mice. Journal of immunology. 2006; 176:6254–6261.

26. Jiang J, Lv HS, Lin JH, Jiang DF, Chen ZK. LTB4 can directly stimulate human osteoclast formation from PBMC independent of RANKL. Artif Cells Blood Substit Immobil Biotechnol. 2005; 33:391–403. [PubMed: 16317958]

27. Garcia C, Boyce BF, Gilles J, Dallas M, Qiao M, Mundy GR, Bonewald LF. Leukotriene B4 stimulates osteoclastic bone resorption both in vitro and in vivo. Journal of bone and mineral research : the official journal of the American Society for Bone and Mineral Research. 1996; 11:1619–1627.

28. Diaz-Gonzalez F, Alten RH, Bensen WG, Brown JP, Sibley JT, Dougados M, Bombardieri S, Durez P, Ortiz P, de-Miquel G, Staab A, Sigmund R, Salin L, Leledy C, Polmar SH. Clinical trial of a leucotriene B4 receptor antagonist, BIIL 284, in patients with rheumatoid arthritis. Annals of the rheumatic diseases. 2007; 66:628–632. [PubMed: 17170051]

29. Tager AM, Dufour JH, Goodarzi K, Bercury SD, von Andrian UH, Luster AD. BLTR mediates leukotriene B(4)-induced chemotaxis and adhesion and plays a dominant role in eosinophil accumulation in a murine model of peritonitis. The Journal of experimental medicine. 2000; 192:439–446. [PubMed: 10934232]

30. Chen ZY, He CY, Kay MA. Improved production and purification of minicircle DNA vector free of plasmid bacterial sequences and capable of persistent transgene expression in vivo. Human gene therapy. 2005; 16:126–131. [PubMed: 15703495]

31. Bouchareychas L, Pirault J, Saint-Charles F, Deswaerte V, Le Roy T, Jessup W, Giral P, Le Goff W, Huby T, Gautier EL, Lesnik P. Promoting macrophage survival delays progression of pre-existing atherosclerotic lesions through macrophage-derived apoE. Cardiovascular research. 2015; 108:111–123. [PubMed: 26092098]

32. Huang WW, Garcia-Zepeda EA, Sauty A, Oettgen HC, Rothenberg ME, Luster AD. Molecular and biological characterization of the murine leukotriene B4 receptor expressed on eosinophils. The Journal of experimental medicine. 1998; 188:1063–1074. [PubMed: 9743525]

33. Spite M, Hellmann J, Tang Y, Mathis SP, Kosuri M, Bhatnagar A, Jala VR, Haribabu B. Deficiency of the leukotriene B4 receptor, BLT-1, protects against systemic insulin resistance in diet-induced obesity. Journal of immunology. 2011; 187:1942–1949.

34. Gheorghe KR, Korotkova M, Catrina AI, Backman L, af Klint E, Claesson HE, Radmark O, Jakobsson PJ. Expression of 5-lipoxygenase and 15-lipoxygenase in rheumatoid arthritis synovium and effects of intraarticular glucocorticoids. Arthritis research & therapy. 2009; 11:R83. [PubMed: 19497113]

35. Subbarao K V, Jala R, Mathis S, Suttles J, Zacharias W, Ahamed J, Ali H, Tseng MT, Haribabu B. Role of leukotriene B4 receptors in the development of atherosclerosis: potential mechanisms. Arteriosclerosis, thrombosis, and vascular biology. 2004; 24:369–375.

36. Saiwai H, Ohkawa Y, Yamada H, Kumamaru H, Harada A, Okano H, Yokomizo T, Iwamoto Y, Okada S. The LTB4-BLT1 axis mediates neutrophil infiltration and secondary injury in experimental spinal cord injury. The American journal of pathology. 2010; 176:2352–2366. [PubMed: 20304963]

37. Hettinger J, Richards DM, Hansson J, Barra MM, Joschko AC, Krijgsveld J, Feuerer M. Origin of monocytes and macrophages in a committed progenitor. Nature immunology. 2013; 14:821–830. [PubMed: 23812096]

38. Misharin AV, Cuda CM, Saber R, Turner JD, Gierut AK, Haines GK 3rd, Berdnikovs S, Filer A, Clark AR, Buckley CD, Mutlu GM, Budinger GR, Perlman H. Nonclassical Ly6C(−) monocytes

drive the development of inflammatory arthritis in mice. Cell reports. 2014; 9:591–604. [PubMed: 25373902]

39. Dal-Secco D, Wang J, Zeng Z, Kolaczkowska E, Wong CH, Petri B, Ransohoff RM, Charo IF, Jenne CN, Kubes P. A dynamic spectrum of monocytes arising from the in situ reprogramming of CCR2+ monocytes at a site of sterile injury. The Journal of experimental medicine. 2015; 212:447–456. [PubMed: 25800956]
40. Hikiji H, Ishii S, Yokomizo T, Takato T, Shimizu T. A distinctive role of the leukotriene B4 receptor BLT1 in osteoclastic activity during bone loss. Proceedings of the National Academy of Sciences of the United States of America. 2009; 106:21294–21299. [PubMed: 19965376]
41. Herrera BS, Ohira T, Gao L, Omori K, Yang R, Zhu M, Muscara MN, Serhan CN, Van Dyke TE, Gyurko R. An endogenous regulator of inflammation, resolvin E1, modulates osteoclast differentiation and bone resorption. British journal of pharmacology. 2008; 155:1214–1223. [PubMed: 18806821]
42. Sanchez-Galan E, Gomez-Hernandez A, Vidal C, Martin-Ventura JL, Blanco-Colio LM, Munoz-Garcia B, Ortega L, Egido J, Tunon J. Leukotriene B4 enhances the activity of nuclear factor-kappaB pathway through BLT1 and BLT2 receptors in atherosclerosis. Cardiovascular research. 2009; 81:216–225. [PubMed: 18852255]
43. Serezani CH, Lewis C, Jancar S, Peters-Golden M. Leukotriene B4 amplifies NF-kappaB activation in mouse macrophages by reducing SOCS1 inhibition of MyD88 expression. The Journal of clinical investigation. 2011; 121:671–682. [PubMed: 21206089]
44. Takami M, Kim N, Rho J, Choi Y. Stimulation by toll-like receptors inhibits osteoclast differentiation. Journal of immunology. 2002; 169:1516–1523.

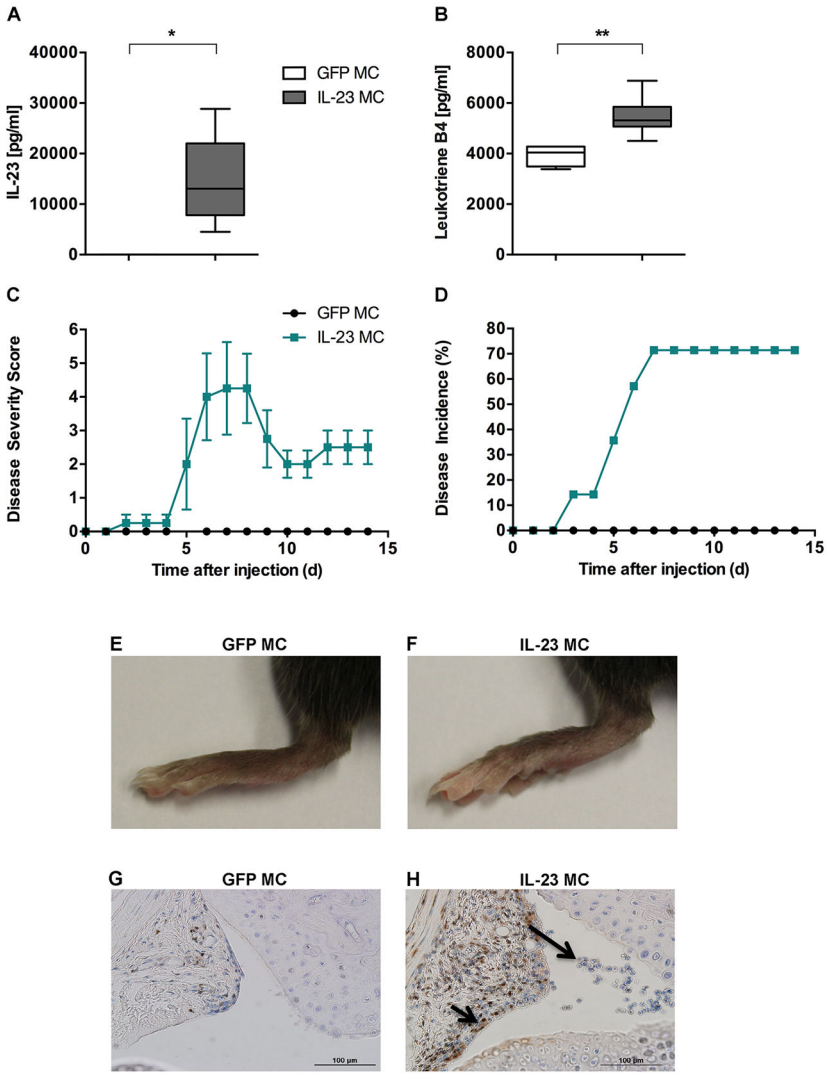

Figure 1. Hydrodynamic delivery of IL-23 MC induces chronic inflammatory arthritis and interacts with LTB4 pathways

Quantification of (**A**) serum IL-23 and (**B**) plasma Leukotriene B4 level by ELISA and EIA in B10.RIII mice after GFP (n=4) or IL-23 MC injection (n=6). Median, interquartile minimum, and maximum range, is depicted by box plots. **C**) Time course of joint swelling and **D**) Incidence of arthritis in B10.RIII mice after GFP (n=3) or IL-23 MC injection (n=5). Vertical bars represent SEM. Representative images of the hind paws of B10.RIII mice injected with GFP MC (**E**) or IL-23 MC (**F**). Representative images of 5-LO immunohistochemical staining (small black arrows) in synovial tissue from B10.RIII mice, 14 days after GFP MC (**G**) or IL-23 MC injection (**H**). Large arrow indicates abundant cellular infiltrate within the synovial membrane. All data are shown as mean ± SEM. *p<0.05,** p<0.01, ***p<0.001 as determined by Mann-Whitney U-test.

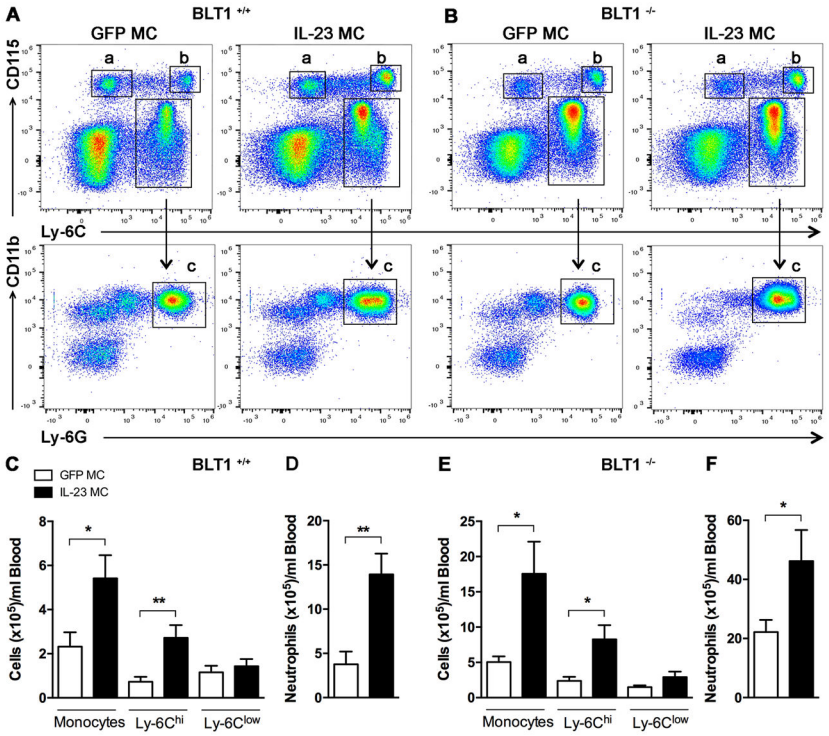

Figure 2. Systemic IL-23 induces myelopoiesis in both BLT1$^{+/+}$ and BLT1$^{-/-}$ mice

Flow cytometric analysis of blood from (**A**) BLT1$^{+/+}$ mice and (**B**) BLT1$^{-/-}$ mice injected with GFP or IL-23 MC. Cells were first visualized on FSC and SSC, followed by exclusion of doublets. Representative dot plots analysis showing the gating strategy that was used to identify monocytes (upper row in **a** and **b**), Ly-6C^{low} (**a**) Ly-6C^{hi} (**b**) monocytes and neutrophils (lower row in **c**). Representative dot plot analysis of one representative experiment of two with similar results are shown. (C) Absolute cell counts of blood monocytes including Ly-6C^{high} and Ly-6C^{low} monocytes and neutrophils (D) in BLT1$^{+/+}$ mice after GFP (n=4) or IL-23 MC injection (n=6). (E) Absolute cell counts of blood monocytes including Ly-6C^{high} and Ly-6C^{low} monocytes and neutrophils (F) in BLT1$^{-/-}$ mice injected with GFP MC (n=7) or IL-23 MC (n=6). All data are shown as mean ± SEM. *p<0.05, **p<0.01 of two independent experiments. Statistical analysis was performed using two-tailed Student's t-test.

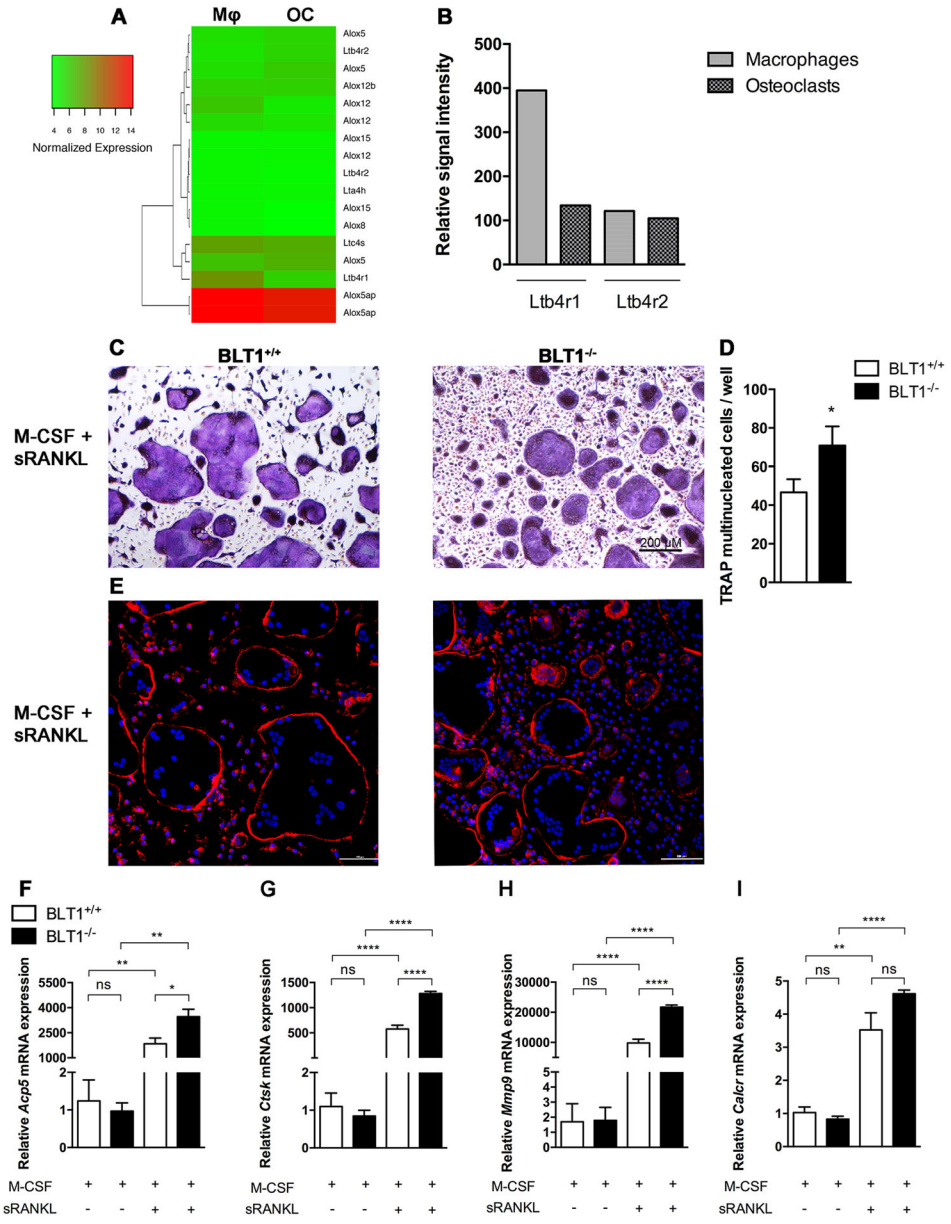

Figure 3. BLT1 deficient mice show increased osteoclast formation

(A) Hierarchical cluster analysis of DNA microarray data obtained from BLT1$^{+/+}$ bone marrow derived macrophages treated with MCSF (Mφ) for 4 days or MCSF and RANKL (OC) for 6 days displaying the differential gene expression patterns of LTB4 synthesis pathway. Columns represent experimental conditions, and rows represent individual genes selected based on fold changes of 2 or more. Green indicates low level of expression, and red indicates high level of expression. The color bar represents expression scale. (**B)** Graphical representation of microarray signal intensities from Ltb4r1 (BLT1) and Ltb4r2 (BLT2) in macrophages and osteoclasts. (**C)** TRAP cytochemical stain and (**D**) number of TRAP positive cells of BLT1$^{+/+}$ and BLT1$^{-/-}$ in four-day cultures of mouse osteoclasts

stimulated with M-CSF and RANKL. Data are shown as mean ± SEM. *p<0.05, Unpaired Student's t-test.

(**E**) Fluorescence photomicrographs of mouse osteoclasts showing the presence of F-actin rings in BLT1$^{+/+}$ and BLT1$^{-/-}$ osteoclasts. Blue: nuclei (DAPI); red: F-actin structures (Phalloidin-TRITC). Representative images of 3 experiments. (**F–I)** qRT–PCR expression analysis for the indicated genes during differentiation of BLT1$^{+/+}$ and BLT1$^{-/-}$ bone marrow cells into osteoclasts at day 4 after RANKL stimulation. Data are presented as a fold change normalized to BLT1$^{+/+}$ M-CSF treated cells (n=3 mice per group). All data are shown as mean ± SEM. *p<0.05, **p<0.01, ***p<0.001, ****p< 0.0001 as determined by a one-way ANOVA with Tukey post hoc test.

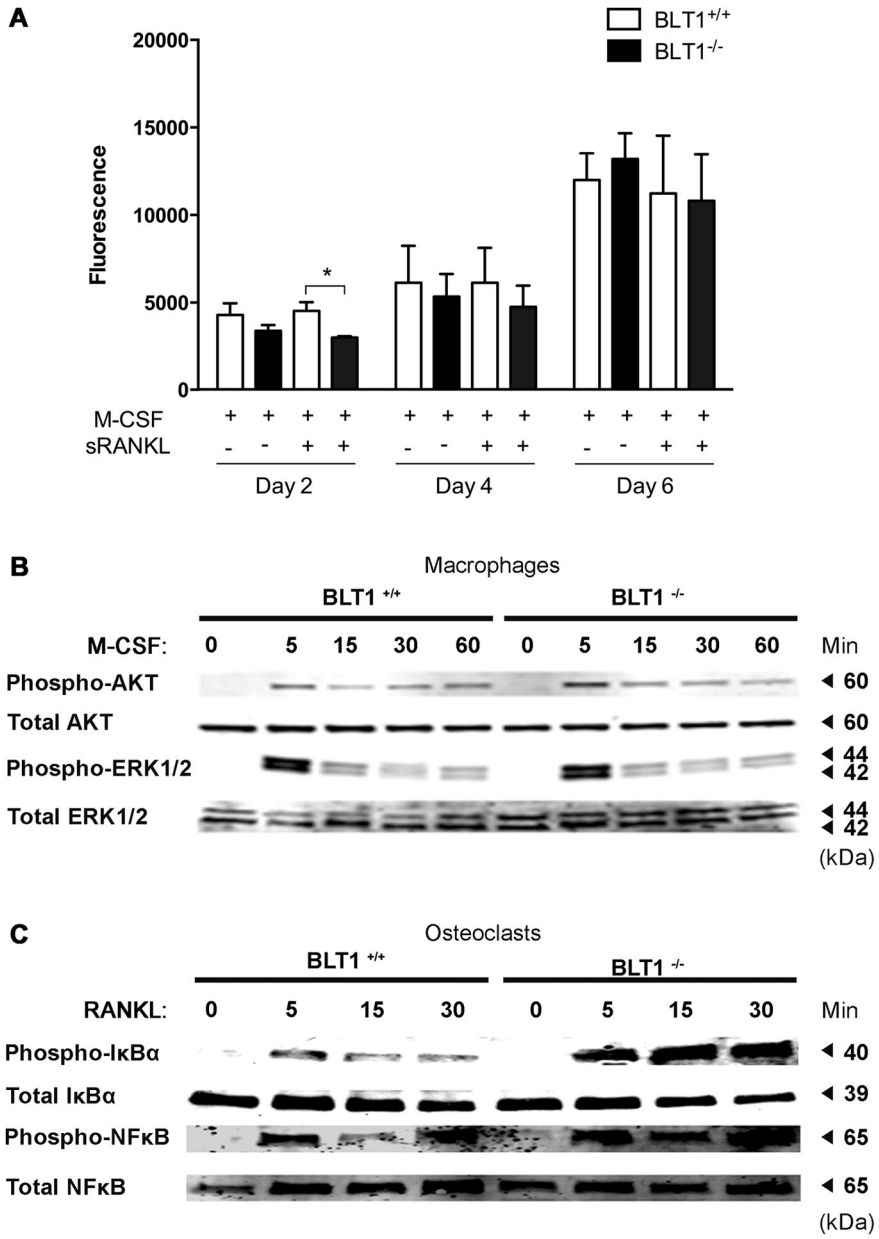

Figure 4. Effect of BLT1 deficiency on macrophage/osteoclast proliferation and differentiation

(**A**) Alamar Blue assay during differentiation of BLT1$^{+/+}$ and BLT1$^{-/-}$ bone marrow cells into osteoclasts at day 2, day 4 and day 6 after RANKL stimulation. (**B**) Western blot analysis of total cell lysates derived from bone marrow macrophage of BLT1$^{+/+}$ and BLT1$^{-/-}$ mice stimulated with M-CSF (100ng/ml) for indicated times and immunoblotted with phospho/total-AKT and phospho/total-ERK1/2 antibodies. (**C**) Western blot analysis of total cell lysates derived from bone marrow macrophage of BLT1$^{+/+}$ and BLT1$^{-/-}$ mice stimulated with RANKL (100ng/ml) for indicated times and immunoblotted with phospho/total-IκBα and phospho/total-NF-κB antibodies.

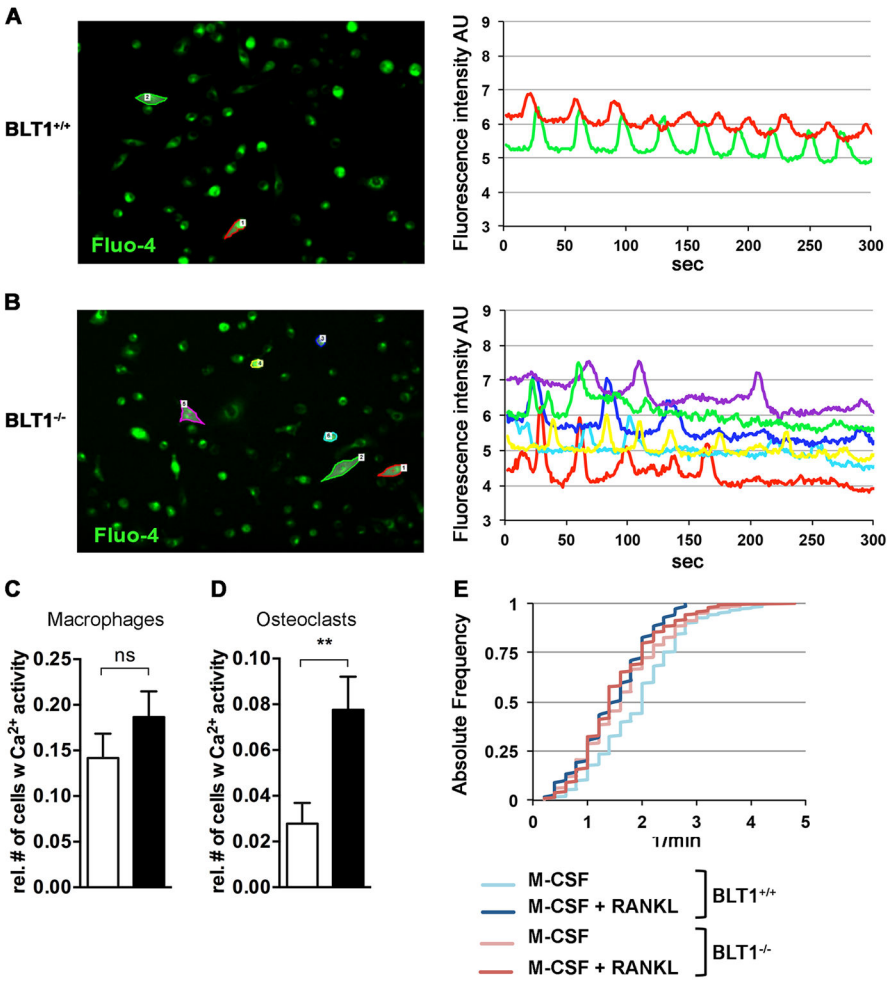

Figure 5. Increased calcium activity in RANKL-stimulated BLT1$^{-/-}$ macrophages

(**A-B**) Left panels: Representative screen shots of time-lapse videos recorded over a period of 300 seconds showing bone marrow macrophages derived from BLT1$^{+/+}$ (**A**) and BLT1$^{-/-}$ (**B**) mice cultured in the presence of M-CSF +/− RANKL for 48 h and loaded with Fluo-4-AM. Outlined cells represent cells exhibiting calcium activity. Right panels: representative plots of oscillation-like patterns of such cells. (**C**) Quantification analysis showing the relative number of macrophages exhibiting calcium activity normalized to the total number of cells per field of view (n=12 per group). Data are shown as mean ± SEM. Unpaired Student's t-test. (**D**) Quantification analysis showing the relative number of osteoclasts exhibiting calcium activity normalized to the total number of cells per field of view (n=18 per group). Data are shown as mean ± SEM. **p<0.01, Mann-Whitney U-test. (**E**) Cumulative distribution of cells showing calcium activity over oscillation frequency (1/min) in respective groups.